

Article

Genome-Wide Identification and Phylogenetic Analysis of TRP Gene Family Members in Saurian

Lin Zhang ^{1,2,*}, Ning Li ^{3,†}, Buddhi Dayananda ⁴, Lihu Wang ⁵, Huimin Chen ^{6,*} and Yunpeng Cao ^{7,*}¹ School of Health and Nursing, Wuchang University of Technology, Wuhan 430223, China² State Key Laboratory of Microbial Technology, Institute of Microbial Technology, Shandong University, Qingdao 266237, China³ College of Food Science, Nanjing Xiaozhuang University, Nanjing 211171, China⁴ School of Agriculture and Food Sciences, The University of Queensland, Brisbane, QLD 4072, Australia⁵ School of Landscape and Ecological Engineering, Hebei University of Engineering, Handan 056038, China⁶ School of Basic Medical Sciences, Hubei University of Chinese Medicine, Wuhan 430065, China⁷ CAS Key Laboratory of Plant Germplasm Enhancement and Specialty Agriculture, Wuhan Botanical Garden, Chinese Academy of Sciences, Wuhan 430074, China

* Correspondence: lzhangss@msn.com (L.Z.); chm1215@hbtcm.edu.cn (H.C.); caoyunpeng@wbgcas.cn (Y.C.)

† These authors contributed equally to this work.

Simple Summary: A total of 251 putative TRPs from saurian are divided into 2 groups, belonging to 6 TRPs subfamilies, excluding the TRPN subfamily. The most conserved proteins of TRP box 1 are located in motif 1, and those of TRP box 2 are located in motif 10. The TRPA and TRPV in saurian tend to be one cluster, as a sister cluster with TRPC, and the TRPM is a root of group I. TRPM, TRPV, and TRPP are clustered into two clades, and TRPP is organized into TRP PKD1-like and PKD2-like. Segmental duplications mainly occur in the TRPM subfamily, and the tandem duplications only occur in the TRPV subfamily. Fifteen sites were under positive selection for TRPA1 and TRPV2 genes. The branch model revealed that positive selection fit the data better than the null model for the genes TRPC5 and TRPV3.



Citation: Zhang, L.; Li, N.; Dayananda, B.; Wang, L.; Chen, H.; Cao, Y. Genome-Wide Identification and Phylogenetic Analysis of TRP Gene Family Members in Saurian. *Animals* **2022**, *12*, 3593. <https://doi.org/10.3390/ani12243593>

Received: 2 November 2022

Accepted: 16 December 2022

Published: 19 December 2022

Publisher's Note: MDPI stays neutral with regard to jurisdictional claims in published maps and institutional affiliations.



Copyright: © 2022 by the authors. Licensee MDPI, Basel, Switzerland. This article is an open access article distributed under the terms and conditions of the Creative Commons Attribution (CC BY) license (<https://creativecommons.org/licenses/by/4.0/>).

Abstract: The transient receptor potential plays a critical role in the sensory nervous systems of vertebrates in response to various mechanisms and stimuli, such as environmental temperature. We studied the physiological adaptive evolution of the TRP gene in the saurian family and performed a comprehensive analysis to identify the evolution of the thermo-TRPs channels. All 251 putative TRPs were divided into 6 subfamilies, except TRPN, from the 8 saurian genomes. Multiple characteristics of these genes were analyzed. The results showed that the most conserved proteins of TRP box 1 were located in motif 1, and those of TRP box 2 were located in motif 10. The TRPA and TRPV in saurian tend to be one cluster, as a sister cluster with TRPC, and the TRPM is the root of group I. The TRPM, TRPV, and TRPP were clustered into two clades, and TRPP were organized into TRP PKD1-like and PKD2-like. Segmental duplications mainly occurred in the TRPM subfamily, and tandem duplications only occurred in the TRPV subfamily. There were 15 sites to be under positive selection for TRPA1 and TRPV2 genes. In summary, gene structure, chromosomal location, gene duplication, synteny analysis, and selective pressure at the molecular level provided some new evidence for genetic adaptation to the environment. This result provides a basis for identifying and classifying TRP genes and contributes to further elucidating their potential function in thermal sensors.

Keywords: TRP gene family; saurian; evolution; genome-wide; thermal sensors

1. Introduction

Ectotherms' body temperature, an important physiological parameter, is essential for the optimal performance of physiological functions within a narrow thermal environment [1–4]. The capacity to maintain body temperature directly indicates the fitness of

individuals [5]. Changes in ambient temperature influence the individuals' physiology, performance, and fitness [6]. The thermally heterogeneous changes, including microhabitats, seasonality, and climate change, influence individuals' body temperature [2]. Individuals employ behavioral or postural adjustments to control their body temperature to avoid harmful extremes [7]. The interactions between ecological and physiological traits directly determine thermal performance, which is the result of selective pressures and evolution [1,8,9]. Changes in ambient temperature influence the individual physiology, altering performance and fitness. To balance the trade-off of the heat exchange between the individuals and their thermal environment, individuals have to evolve some reliable thermosensory proteins, to rapidly respond with physiology or behavior to the complex spatial and temporal changes in the thermal environment [10]. The ability to sense environmental and internal temperatures is a prerequisite for the evolution of thermoregulation [11]. Hence, individuals require a sophisticated physiological system to sense the ambient temperature for survival [12].

Ectotherms employed sensory neurons in the peripheral nervous system, as temperature-sensitive ion channels [13]. Transient receptor potential (TRPs) consists of Ca^{2+} permeable non-selective cation channels, which function in numerous physiological processes and homeostatic functions [14]. This response is due to a signaling cascade that produces a transitory change in receptor potential [15,16]. The TRPs were divided into seven subfamilies based on their amino acid sequences and structures, as TRPA (Ankyrin), TRPC (Canonical), TRPM (Melastatin), TRPML (Mucolipin), TRPN (Nomp), TRPP (Polycystin), and TRPV (Vanilloid) [17]. Depending on the variations in the luminal/extracellular domain between transmembrane helix 1 (S1) and S2 [18,19], the seven subfamilies are recognized and divided into group I (TRPA/C/M/N/V) and group II (TRPML and TRPP). The TRPP subfamily is an ancient member of the TRPs [19]. During the evolution of the TRPs, six subfamilies have been observed in vertebrates [20], except TRPN, which only occurs in zebrafish and invertebrates [21]. The thermo-TRPs, of the TRP channels activated by temperature, are divided into heat-sensitive proteins (TRPV1-4) [22] and cold-sensitive proteins (TRPM8, TRPC5, and TRPA1) [23–25]. The TRPV1, a classic thermo-TRP, is directly activated by high temperatures (≥ 43 °C) in humans [26]. The TRPM8 regulates thermoregulation as it relates to cold temperature sensation in lizards because it does not participate in regulating warm temperature behaviors such as gaping [2]. To adapt to thermal niches, some changes in TRP improve thermal perception and responses in the individual's large-scale evolution. All these findings indicate the important roles of TRP channels in the different environmental stimuli. However, to date, most of the research on TRP proteins has mostly been performed on mammals.

In reptiles, TRPs play a key role in interpreting thermal stimuli to rapidly and accurately sense the environment around them [11,13,27,28]. Inhibition of *TRPV1* and *TRPM8* by the blocker capsaizepine in *Crocodylus porosus* abolished the typical ectotherms shuttling behavior and led to significantly altered body temperature patterns [11]. It indicates that the function of TRPs in reptiles for thermoregulation is similar to that in mammals. In *Takydromus tachydromoides*, cold treatment reduced *TRPV4* expression in the brain, tongue, heart, lungs, and muscles in the hibernation species, but levels of *TRPV4* mRNA in the skin remained unaffected after entering hibernation and cold treatment [29]. In *Mauremys reevesii*, the embryos moved toward a mild heat source when the ambient temperature was above 29 °C due to TRPA1 activation, but embryos moved away from the noxious heat source when the ambient temperature was above 33 °C due to TRPV1 activation [30]. *Thermophilis baileyi* exhibited species-specific temperature-sensing molecular strategies (amino acid replacements) in the *TRPA1*, which did not influence the temperature-response margin but increased the heat sensitivity [31]. Moreover, previous studies have shown that thermosensitive gating in a given channel is species-specific, and multiple channels act together to sense the thermal environment [10]. However, there is little information on the TRP proteins' gene family in reptiles.

In this study, to test the physiological adaptive evolution of the TRP gene family in saurian, we performed a comprehensive analysis of the genome sequence data of eight saurian species and identified the TRP protein gene family. We analyzed their phylogenetic relationships, conserved motifs, gene structure, and gene duplication. To improve the understanding of the evolution of the thermo-TRP channels in saurian, we performed selective pressure analysis on thermo-TRPs to identify the positive selection.

2. Materials and Methods

2.1. Identification of TRP Gene Family in Saurian

We downloaded the saurian genomes (Table S1), including those of *Anolis carolinensis*, *Gekko japonicus*, *Lacerta agilis*, *Podarcis muralis*, *Pogona vitticeps*, *Sceloporus undulatus*, *Sphaerodactylus townsendi*, and *Zootoca vivipara*, from the NCBI database (<https://www.ncbi.nlm.nih.gov/genome>, accessed on 22 July 2022). We employed TBtools [32] to generate the Hidden Markov Model (HMM) of TRPs based on *Homo sapiens* from HGNC (<https://www.genenames.org>, accessed on 22 July 2022), *Xenopus tropicalis* from Xenbase (<https://www.xenbase.org/entry/>, accessed on 22 July 2022), and *Danio rerio* from ZFIN (<https://www.zfin.org/>, accessed on 22 July 2022) to identify the TRP members based on the HMM of TRPs by using HMMER3 software [33]. To avoid missing probable TRP members, we used a BLASTp algorithm-based search using molluscan TRPs amino acid sequences as queries with a cutoff e-value $\leq 1e-5$ [34]. Overlapping genes were manually removed. All candidate TRP genes were filtered by using the NCBI Conserved Domain Database (CDD, <https://www.ncbi.nlm.nih.gov/Structure/cdd/cdd.shtml>, accessed on 22 July 2022) [35,36] and Multiple EM for the Motif Elicitation (MEME) online tool (<http://meme-suite.org/tools/meme>, accessed on 22 July 2022) [37]. The MEME was set with the following parameters: any number of repetitions, a maximum of 10 motifs, and an optimum motif width of 6–50 residues [38], and MEME online was employed to analyze the motif structure of TRP proteins. The Gene Structure View (Advanced) was employed for the visualization of conserved domains and motifs in TBtools [32]. Next, using TBtools, we detected the exact chromosomal locations of all TRP genes through a BLAST search of the genome sequences. Due to the association with the highly conserved region of 23–25 amino acids C-terminal to the transmembrane domains [39], we ran a comparative analysis of the conserved domain in saurian.

2.2. Phylogenetic Analysis

The TRPs were aligned using MAFFT [40] and implemented in PhyloSuite [41]. According to the best model as implemented in IQ-TREE2, the maximum likelihood (ML) tree was computed and built with a bootstrap test (5000 replicates) and the SH-aLRT test (1000 random addition replicates) [42]. Phylogenetic consensus trees were edited by using iTOL (<https://itol.embl.de>, accessed on 22 August 2022) [43].

2.3. Chromosome Locations and Synteny Analysis

The chromosomal locations of TRP genes, except for *Gekko japonicus* and *Pogona vitticeps*, were obtained from general feature format files. Gene location visualization from the GFF was used to map the distribution of TRP genes. To identify the orthologous genes among eight saurian genomes, we used OrthoFinder [44], and MCSanX was employed to conduct colinearity analyses of all TRPs between and within species [45]. Circos was used to visualize the colinear relationships of TRPs [46] and the distribution of these genes on the chromosomes in TBtools.

2.4. Selective Pressure Analysis

Based on the previous research [12,47], we selected seven genes, including TRPA1, TRPM8, TRPC5, and TRPV1-4, to analyze the selection pressure in the eight saurian genomes, and then calculated the proportions of the non-synonymous (dN)/synonymous (dS) evolutionary rate (ω) using EasyCodeML v1.12 [48] to represent the selective selection.

Different ω values indicated a different type of selection: $\omega > 1$ shows the positive selection, $\omega = 1$ represents the neutral selection, and $\omega < 1$ represents the purifying selection [49]. We employed a fast unconstrained Bayesian approximation (FUBAR) on the Datamonkey website to detect the positive selection implemented [50]. The analysis was calculated based on the site model (M8a vs. M8) [51] and branch model (two ratios vs. one ratio) with the likelihood ratio test (LRT) threshold of $p < 0.05$, elucidating adaptation signatures within the genome. Amino acid sites under positive selection were detected using Bayesian empirical bayes (BEB) inference, with an 80% posterior probability cutoff [52].

3. Results

3.1. TRP Genes in Saurian

A total of 32, 30, 30, 33, 27, 28, 28, and 31 TRPs were identified in *A. carolinensis*, *G. japonicus*, *L. agilis*, *P. muralis*, *P. vitticeps*, *S. undulatus*, *S. townsendi*, and *Z. vivipara*, respectively (Figure 1 and Table S1). Ten conserved motifs were identified using MEME in saurian (Figure S1). Motif 2 was present in each saurian TRP protein, and the TRPM included all 10 motifs. No TRPN proteins were found in the eight saurian genomes (Figure 1). The most conserved proteins of TRP box 1 were located in motif 1, and those of TRP box 2 were located in motif 10.

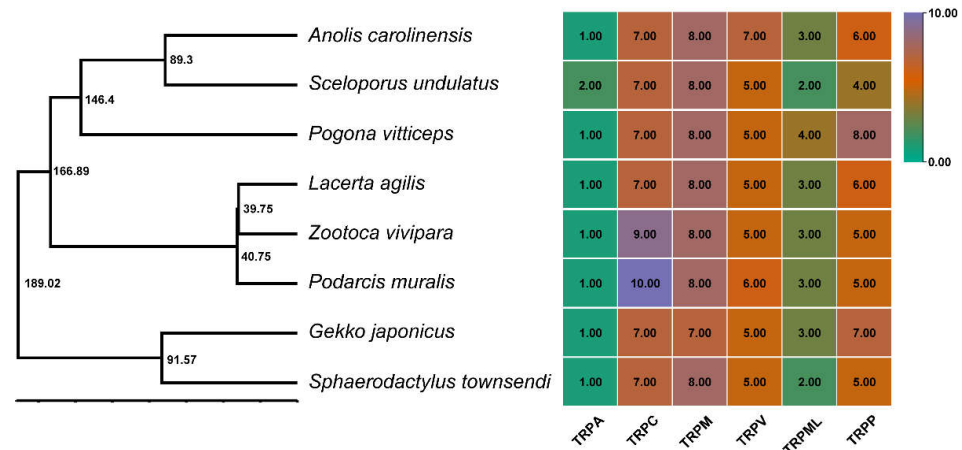


Figure 1. Species tree of eight saurian and TRP numbers of each species. The time tree of the eight saurian was built by the TIMETREE 5 (left, the number is the divergence time), and the numbers of the TRP family detected in each species were listed accordingly (right).

3.2. Phylogenetic Relationships of TRPs in Saurian Genomes

To explore the evolutionary differences and origins of these TRP protein families in saurian, we further analyzed the molecular histories of these genes. We performed maximum-likelihood (ML) analysis on the amino acid sequences of all 251 TRPs using the ML method with 1000 bootstrap replicates (Figure 2). The TRPs were clustered into six subgroups (TRPA, TRPC, TRPP, TRPM, TRPML, and TRPV), which belong to two monophyletic clades as group I and group II. Group I contained four subfamilies, TRPA, TRPC, TRPM, and TRPV, and group II contained two subfamilies, TRML and TRPP, respectively. Phylogenetic analysis indicated that TRPA and TRPV in saurian tended to be one cluster, as the sister cluster with TRPC, and TRPM is the root of group I. The TRPM, TRPV, and TRPP proteins clustered into two clades (Figure 2) and TRPM proteins contained the α TRPM clade (including TRPM3, TRPM1, TRPM6, and TRPM7) and the β TRPM clade (including TRPM4, TRPM5, TRPM2, and TRPM8). TRPV1, TRPV2, TRPV3, and TRPV4 belonged to TRPV protein group I, and the TRPV protein group II contained TRPV5 protein and TRPV6 proteins, which were annotated as TRPV 5/6. TRPP was organized into two clades: TRPP1-like (including TRPPREJ, TRPP1L2, and TRPP1L3) and TRPP2-like (including TRPP2, TRPP2L1, and TRPP2L2).

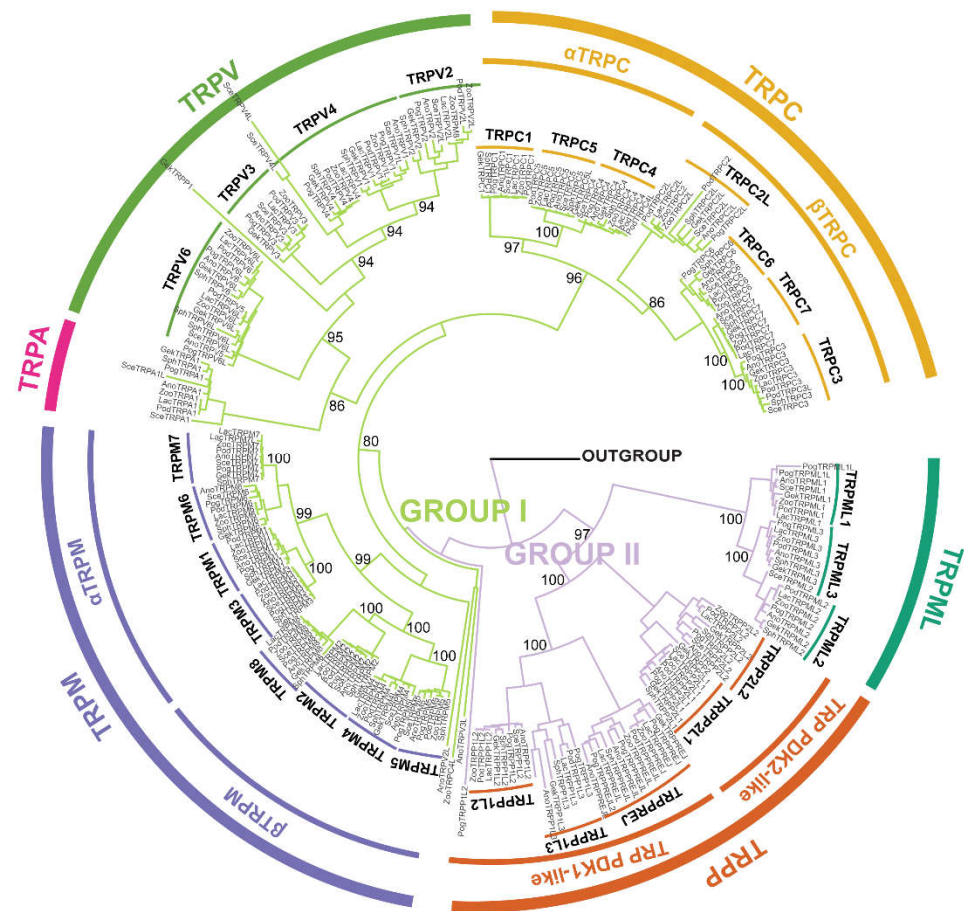


Figure 2. Analysis of the maximum likelihood (ML) tree of TRPs in saurian. Moderate green and grayish violet represent group I and group II, respectively.

3.3. Syntenic Analysis of TRPs in Saurian Genomes

To further identify the orthologous relationships and evolutionary origins of TRPs in saurian, we identified 737 orthologous gene pairs (Table S3). We investigated the synteny among six saurian genomes with chromosome-level genomes using MCScanX, and the data showed that high-level microsynteny was maintained among the saurian genomes (Figure 3). There was a one-to-one correspondence between the gene lineages and syntenic orthologous groups (Figure S2). The TRPs from saurian contributed at least one TRP to each subfamily. In our study, most members of the TRP family were distributed on chromosomes (Figure S3 and Table S4). Based on the results of the syntenic analysis, the segmental duplications (SD) and tandem duplications (TD) were the TRP duplication types in all genomes (Figure 4), but the TRPs did not experience duplication events in *A. carolinensis* (Figure 4). The SD mainly occurred in the TRPM subfamily, and TD only occurred in the TRPV subfamily. There was only one SD in *S. undulatus* (rna-XM_042476030.1 vs. rna-XM_042451064.1), two SD in *L. agilis* (rna-XM_033163651.1 vs. rna-XM_033166883.1 and rna-XM_033160619.1 vs. rna-XM_033140165.1), *P. muralis* (rna-XM_028749274.1 vs. rna-XM_028706666.1 and rna-XM_028728955.1 vs. rna-XM_28718097.1), and *Z. vivipara* (rna-XM_035131044.1 vs. rna-XM_035099594.1 and rna-XM_035137878.1 vs. rna-XM_035104957.1), and three SD in *S. townsendi* (rna-XM_048513883.1 vs. rna-XM_048519142.1, rna-XM_048508742.1 vs. rna-XM_048487239.1, and rna-XM_048519624.1 vs. rna-XM_048503482.1), respectively (Figure S4). There was only one TD in *S. townsendi* (rna-XM_048504402.1 vs. rna-XM_048504571.1), two TD in *S. undulatus* (rna-XM_042442354.1 vs. rna-XM_042442355.1 and rna-XM_042447702.1 vs. rna-XM_042452285.1), three TD in *P. muralis* (rna-XM_028708247.1 vs. rna-XM_028708248.1, rna-XM_028708530.1 vs. rna-XM_028708708.1, and rna-XM_028712426.1 vs. rna-XM_028712789.1) and *Z. vivipara* (rna-XM_035141029.1 vs. rna-XM_035097275.1, rna-XM_035139054.1 vs.

rna-XM_035139047.1, and rna-XM_035139316.1 vs. rna-XM_035139320.1), and four TD in *L. agilis* (rna-XM_033145813.1 vs. rna-XM_033145814.1, rna-XM_033171541.1 vs. rna-XM_033172593.1, rna-XM_033172595.1 vs. rna-XM_033171884.1, and rna-XM_033173257.1 vs. rna-XM_033173677.1), respectively.

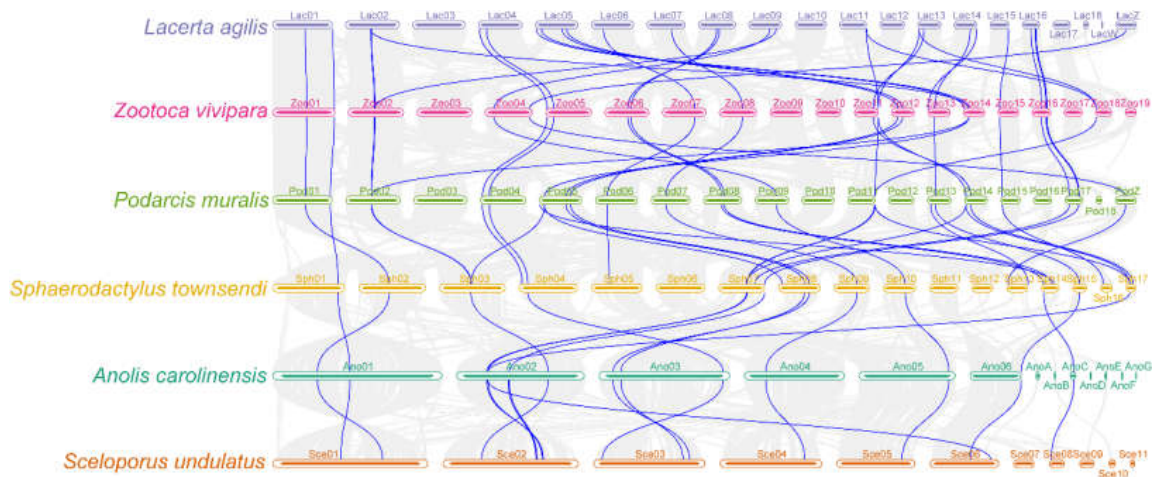


Figure 3. Synteny analysis of *TRP* genes among inter-genomes of saurian. The gray line in the background shows colinear blocks in the six saurian genomes, and the blue line highlights colinear *TRP* pairs.

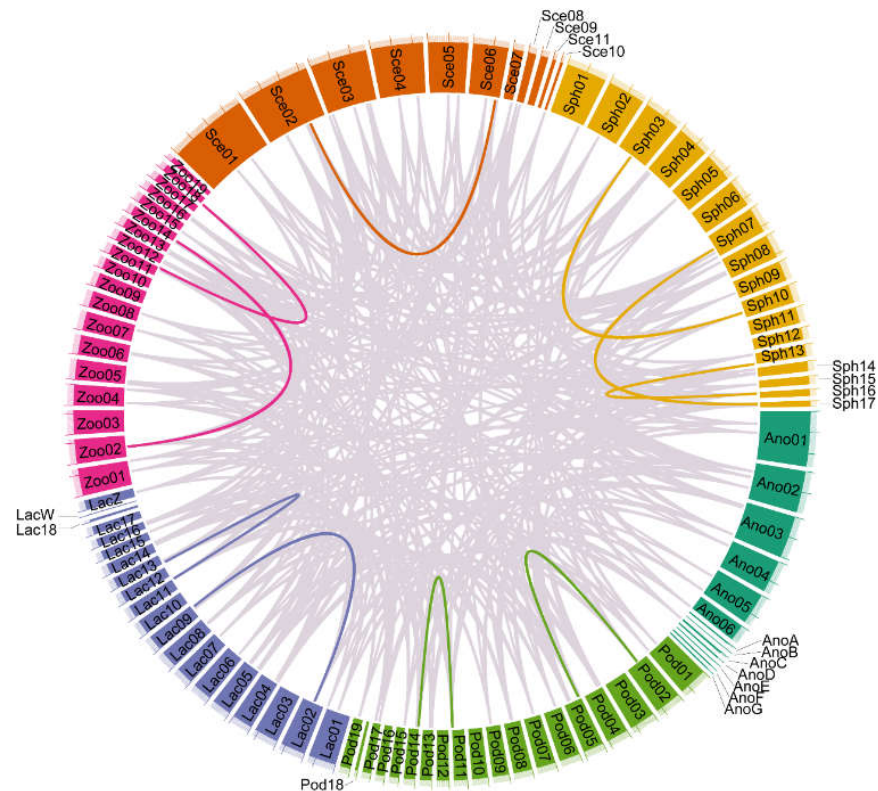


Figure 4. Colinear region of the *TRP* gene of saurian. The gray lines represent all the colinear blocks in *TRP* gene pairs among species, while the highlight-colored lines represent *TRP* gene pairs subjected to segmental duplication within species. Chromosome numbers are shown at the bottom of each chromosome.

3.4. Selective Pressure Analysis in Saurian TRP Gene

To determine whether the individual codons in each gene were subjected to positive selection, we used the site model (M8a vs. M8) in the dataset. The results showed that the M8 model, which included positive selection, fit the data better than the neutral model M8a. Specifically, the M8 model detected 15 sites to be under positive selection at *TRPA1* and *TRPV2* genes (Table 1 and Figure 5), most of which were located in the coil of *TRPA1* and *TRPV2* genes. Significant evidence of positive selection was further identified using the FUBAR model implemented in Datamonkey. Additionally, FUBAR also identified 13 sites in these two genes under diversifying selection with a posterior probability > 0.8.

Table 1. Positive selection at amino acid sites of saurian TRPs.

	PAML			Datamonkey
	−2ΔlnL	Site Model	ω Value	FUBAR
<i>TRPA1</i>	10.58	4, 17, <u>147</u> , <u>182</u> , <u>216</u> , <u>750</u> , <u>757</u> , 828, 873, <u>1110*</u> , <u>1112*</u>	3.18	92, 115, <u>147</u> , 174, <u>182*</u> , <u>216*</u> , <u>232</u> , <u>750</u> , <u>757</u> , <u>1110*</u> , <u>1112</u>
<i>TRPV2</i>	6.28	<u>275</u> , 715, <u>717*</u> , <u>735*</u>	4.35	38, <u>275</u> , 563

Note: Positively selected sites inferred by both methods are underlined. *: Selective pressure > 0.9.

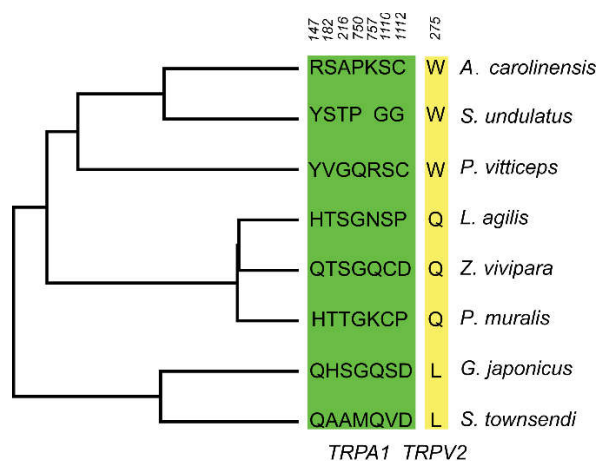


Figure 5. Amino acid changes in selected sites across the saurian phylogeny. Amino acid changes occurred in genes *TRPA1* (green) and *TRPV2* (yellow). The numbers represent the amino acid positions in the genes *TRPA1* and *TRPV2*.

A branch model with two ratios was used to explore whether saurian with daily activity rhythms (classified into two groups, i.e., diurnal and nocturnal saurian) evolved under different evolutionary pressures. The results revealed that the model that included positive selection fit the data better than their null model at genes *TRPC5* (two ratios vs. one ratio: $p = 0.025$) and *TRPV3* (two ratios vs. one ratio: $p = 0.032$) (Table 2).

Table 2. Log likelihood and omega values estimated under the branch model of *Gekko japonicus* on TRP genes.

	Model	−lnL	−2ΔlnL	p-Value	ω Value	
					Background	Foreground
<i>TRPC5</i>	Two ratios	−8267.20	4.99	0.025	0.03	0.07
	One ratio	−8269.69				
<i>TRPV3</i>	Two ratios	−7736.71	4.62	0.032	0.06	0.11
	One ratio	−7739.02				

4. Discussion

In this study, all 251 identified putative *TRPs* with 6 subfamilies, except *TRPN*, were identified from 8 saurian genomes. This study is the first study to characterize the repertoire and evolutionary patterns of the *TRP* gene family in saurian. All *TRPs* were highly conserved in their sequences and structural features. Based on the selective pressure analysis and the activity time of the species, we hypothesized that *TRPA1*, *TRPV2*, *TRPV3*, and *TRPC5* are the thermo-TRP channels of saurian. Our results provide a novel view of the saurian thermal sensor system at the molecular level.

Over the past two decades, more and more species were sequenced since the genome of *A. carolinensis* was reported, and genomic data provide us with convenient conditions for analyzing evolution, including gene structure, chromosome location, gene duplication, synteny analysis, and selective pressure. Genome-wide screening revealed 32, 30, 30, 33, 27, 28, 28, and 31 *TRPs* in *A. carolinensis*, *G. japonicus*, *L. agilis*, *P. muralis*, *P. vitticeps*, *S. undulatus*, *S. townsendi*, and *Z. vivipara*, respectively (Figure 1 and Table S2). The *TRPs* belonged to six *TRP* subfamilies, except for the *TRPN* subfamily. The *TRPN* members are only present in worms, flies, and zebrafish, except in Antarctic fish [10], mammals [39], and saurian. Reptiles share a common ancestor with mammals and have an important amniote phylogeny position [53]. The number of members of each *TRP* subfamily is relatively more stable in vertebrates than in invertebrates, but there are more *TRPP*-like genes in saurian (Figure 1, right). We found a highly conserved motif named motif 2 in all saurian *TRP* genes. The most conserved portions of the *TRP* domain were identified as the *TRP* boxes 1 and 2 [39], and the results indicated that boxes 1 and 2 were located in motif 1 and motif 10, respectively.

The results showed that the complement of *TRPs* in saurian was similar to that in mammals. The finding supports those of recent analyses of the evolutionary history of *TRP*. In the phylogenetic analysis, we restructured the initial reliability phylogenetic relationship with the high topology consistency of *TRPs*, and further divided these *TRPs* into two groups, which supported the previous results in the literature that members of the *TRPs* are divided into group I and group II [10,54], and the *TRPP* is located at the root of the ML tree, supporting the *TRPP* subfamily as the ancestor of *TRP*, where the members of the *TRPP* subfamily extend from yeast to mammals [19]. *TRPM* proteins are divided into the α *TRPM* and β *TRPM*. The β *TRPM* clade contains the *TRPM2*, *TRPM4*, *TRPM5*, and *TRPM8*, where the *TRPM2*, *TRPM4*, and *TRPM5* are activated by heat, but the *TRPM8* responds to cold temperatures [55]. *TRPV* proteins belong to two groups that assist with this function, *TRPV1-4* proteins are defined as thermosensitive [46], and *TRPV5/6* proteins' function is to maintain Ca^{2+} homeostasis [47]. In lizards, *TRPP* channels are organized into PKD1-like and PKD2-like, except for the brivido subfamily, which differs from the previous studies [54,56].

Moreover, the syntenic analysis showed the number of homology pairs within and/or among species, but the *TRPs* have not experienced the duplication event in *A. carolinensis*. Gene duplication events, such as large-scale duplication (whole-genome duplication or segmental duplication) and tandem duplication, are the main drivers for the generation of novel genes. Large-scale duplication events play a key role in gene family evolution, and tandem duplication does not increase the number of conserved genes [57]. In saurian, the SD mainly occurs in the *TRPM* subfamily, but the TD only occurs in the *TRPV* subfamily. *TRPM* and *TRPV* proteins clustered into two clades, which appears to be due to the ancestral saurian genome duplication, and the event is still observed in fish [10]. The number of duplicated gene pairs in *TRPs* (from 3 to 6, including SD and TD) did not correlate with the genome size and chromosome number in saurian (Figure S3). It is similar in the genome size and chromosome number in saurian, but the number of colinear *TRP* gene pairs varied among species, associated with the phylogenetic site.

The vulnerability of lizards to climate warming depends on the sensitivity of the individuals to temperature variation [7], which increases the risk of population decline and extinction [58]. However, the diel activity pattern reflects the capacity of adaptation

to the variable environment [59], in which the ambient temperature at night is lower than that during the daytime. The ancestral state of geckos is nocturnal, except for *Phelsuma* and *Lygodactylus* in Gekkonidae and Sphaerodactylidae species [60]. Hence, most geckos have lower body temperatures than diurnal species [61,62], reducing the metabolic rate and metabolic by-products as well as oxidative damage [63]. In this study, the selection analysis showed significant evidence of positive selection, including *TRPA1*, *TRPC5*, *TRPV2*, and *TRPV3* in saurian (Tables 1 and 2). In vertebrates, *TRPV1*'s physiological role in sensing noxious high temperatures is well-conserved among vertebrate species [12]. *TRPC5* and *TRPM8* were identified as cold-relative genes [24,64]. In lizard (*Takydromus tachydromoides*) and snake (*Elaphe quadrivirgata*), *TRPV4* in the skin may act as an environmental temperature sensor throughout the reptilian lifecycle [32]. In *C. porosus*, hot-sensing *TRPV1* and cold-sensing *TRPM8* have the potential to act as internal and external temperature sensors, respectively [11].

5. Conclusions

In this study, all 251 putative *TRPs* were divided into 6 subfamilies, except *TRPN*, from 8 saurian genomes, such as *A. carolinensis*, *G. japonicus*, *L. agilis*, *P. muralis*, *P. vitticeps*, *S. undulatus*, *S. townsendi*, and *Z. vivipara*. The results provided a comprehensive analysis of the subfamily classification, gene structure, chromosomal location, gene duplication, synteny analysis, and selective pressure of *TRPs* in saurian and provided new evidence for the physiological adaptive evolution of environmental changes. This investigation provides a basis for identifying and classifying *TRP* genes and contributes to elucidating their potential function in thermal sensors, facilitating future functional characterization of thermo-*TRPs* and providing important clues for saurian thermal sensors.

Supplementary Materials: The following supporting information can be downloaded at: <https://www.mdpi.com/article/10.3390/ani12243593/s1>, Figure S1: Phylogenetic relationships, gene structure, and motif distributions of saurian *TRP* genes. Figure S2: Analysis of ML tree and orthologous gene pairs among the saurian. The different color links suggested orthologous gene relationships of different saurian. Figure S3: Distribution of *TRP* gene pairs within species. The gray lines represent all the colinear blocks in gene pairs within species, while the red lines represent *TRP* gene pairs subjected to segmental duplication within species. Chromosome numbers are shown at the bottom of each chromosome. Table S1: List of saurian genomes and *TRP* gene sequences information in this study. Table S2: The link between gene ID and gene symbol. Table S3: Duplicated *TRP* gene pairs in saurian. Table S4: The divergence between duplicated *TRP* gene pairs in saurian.

Author Contributions: Conceptualization, L.Z. and Y.C.; data curation, L.Z. and N.L.; formal analysis, L.Z. and Y.C.; funding acquisition, L.Z., N.L., and H.C.; investigation, L.Z. and N.L.; methodology, L.Z., L.W., and Y.C.; project administration, L.Z.; resources, N.L.; software, L.Z. and L.W.; supervision, L.Z. and H.C.; validation, L.Z., H.C., and N.L.; visualization, L.Z.; writing—original draft preparation, L.Z., N.L., and H.C.; writing—review and editing, L.Z., B.D., and Y.C. All authors have read and agreed to the published version of the manuscript.

Funding: This research was funded by the National Natural Science Foundation of China (31800337), the Funds for Distinguished Young Scholars of Hubei University of Chinese Medicine (2022ZZXJ003), the Research Start-up Fund of Hubei University of Chinese Medicine, the Funds for the “14th Five-Year” Excellent Discipline Team of Hubei University of Chinese Medicine, the State Key Laboratory of Microbial Technology Open Projects Fund (M2021-18), and the National Famous Old Chinese Medicine Experts Liu Hegang Inheritance Studio Project (G.TCM.R.J.H.[2022]75).

Institutional Review Board Statement: Not applicable.

Informed Consent Statement: Not applicable.

Data Availability Statement: Publicly available datasets were analyzed in this study. This data can be found here: *Anolis carolinensis* [AnoCar2.0], *Gekko japonicus* [Gekko_japonicus_V1.1], *Lacerta agilis* [rLacAgi1.pri], *Podarcis muralis* [PodMur_1.0], *Pogona vitticeps* [pvi1.1], *Sceloporus undulatus* [SceUnd_v1.1], *Sphaerodactylus townsendi* [MPM_Stown_v2.3], and *Zootoca vivipara* [UG_Zviv_1].

Acknowledgments: We wish to thank the anonymous reviewers and the editor of the journal for their valuable comments.

Conflicts of Interest: The authors declare no conflict of interest.

References

1. Angilletta, M.J. *Thermal Adaptation: A Theoretical and Empirical Synthesis*; Oxford University Press: New York, NY, USA, 2009.
2. Black, I.R.G.; Berman, J.M.; Cadena, V.; Tattersall, G.J. Behavioral thermoregulation in lizards: Strategies for achieving preferred temperature. In *Behavior of Lizards: Evolutionary and Mechanistic Perspectives*; Bels, V.L., Russell, A.P., Eds.; CRC Press: Boca Raton, FL, USA, 2019; pp. 13–46.
3. Fernández-Rodríguez, I.; Barroso, F.M.; Carretero, M.A. An integrative analysis of the short-term effects of tail autotomy on thermoregulation and dehydration rates in wall lizards. *J. Therm. Biol.* **2021**, *99*, 102976. [[CrossRef](#)] [[PubMed](#)]
4. Mota-Rojas, D.; Gonçalves, C.; de Mira, A.; Martínez-Burnes, J.; Gómez, J.; Hernández-Ávalos, I.; Casas, A.; Domínguez, A.; José, N.; Bertoni, A.; et al. Efficacy and function of feathers, hair, and glabrous skin in the thermoregulation strategies of domestic animals. *Animals* **2021**, *11*, 3472. [[CrossRef](#)] [[PubMed](#)]
5. Warner, D.A. Fitness consequences of maternal and embryonic responses to environmental variation: Using reptiles as models for studies of developmental plasticity. *Integr. Comp. Biol.* **2014**, *54*, 757–773. [[CrossRef](#)] [[PubMed](#)]
6. Kern, P.; Cramp, R.L.; Franklin, C.E. Physiological responses of ectotherms to daily temperature variation. *J. Exp. Biol.* **2015**, *218*, 3068–3076.
7. Zhang, L.; Dayananda, B.; Xia, J.-G.; Sun, B.J. Editorial: Ecophysiological analysis of vulnerability to climate warming in ectotherms. *Front. Ecol. Evol.* **2022**, *11*, 946836. [[CrossRef](#)]
8. Bodensteiner, B.L.; Audelo-Cantero, G.A.; Arietta, A.Z.A.; Gunderson, A.R.; Muñoz, M.M.; Refsnider, J.M.; Gangloff, E.J. Thermal adaptation revisited: How conserved are thermal traits of reptiles and amphibians? *J. Exp. Zool. A* **2021**, *335*, 173–194. [[CrossRef](#)]
9. Telemeco, R.S.; Gangloff, E.J. Introduction to the special issue—Beyond CT_{MAX} and CT_{MIN} : Advances in studying the thermal limits of reptiles and amphibians. *J. Exp. Zool. A* **2021**, *335*, 5–12. [[CrossRef](#)]
10. York, J.M.; Zakon, H.H. Evolution of transient receptor potential (TRP) ion channels in Antarctic fishes (Cryonotothenioidea) and identification of putative thermosensors. *Genome Biol. Evol.* **2022**, *14*, evac009. [[CrossRef](#)]
11. Seebacher, F.; Murray, S.A. Transient receptor potential ion channels control thermoregulatory behaviour in reptiles. *PLoS ONE* **2007**, *2*, e281. [[CrossRef](#)]
12. Saito, S.; Tominaga, M. Functional diversity and evolutionary dynamics of thermoTRP channels. *Cell Calcium* **2015**, *57*, 214–221. [[CrossRef](#)]
13. Akashi, H. Thermal sensitivity of heat sensor TRPA1 correlates with temperatures inducing heat avoidance behavior in terrestrial ectotherms. *Front. Ecol. Evol.* **2021**, *9*, 583837. [[CrossRef](#)]
14. Nilius, B.; Owsianik, G. The transient receptor potential family of ion channels. *Genome Biol.* **2011**, *12*, 218. [[CrossRef](#)] [[PubMed](#)]
15. Vangeel, L.; Voets, T. Transient receptor potential channels and calcium signaling. *Cold Spring Harb. Perspect. Biol.* **2019**, *11*, a035048. [[CrossRef](#)] [[PubMed](#)]
16. Zhang, Z.M.; Wu, X.L.; Zhang, G.Y.; Ma, X.; He, D.X. Functional food development: Insights from TRP channels. *J. Funct. Foods* **2019**, *56*, 384–394. [[CrossRef](#)]
17. Montell, C.; Birnbaumer, L.; Flockerzi, V.; Bindels, R.J.; Zhu, M.X. A Unified nomenclature for the superfamily of TRP cation channels. *Mol. Cell* **2002**, *9*, 229–231. [[CrossRef](#)]
18. Fine, M.; Li, X.; Dang, S. Structural insights into group II TRP channels. *Cell Calcium* **2020**, *86*, 102107. [[CrossRef](#)]
19. Palmer, C.P.; Aydar, E.; Djamgoz, M.B.A. A microbial TRP-like polycystic-kidney-disease-related ion channel gene. *Biochem. J.* **2005**, *387*, 211–219. [[CrossRef](#)]
20. Peng, C.; Yang, Z.; Liu, Z.; Wang, S.; Yu, H.; Cui, C.; Hu, Y.; Xing, Q.; Hu, J.; Huang, X.; et al. A systematical survey on the TRP channels provides new insight into its functional diversity in Zhikong scallop (*Chlamys farreri*). *Int. J. Mol. Sci.* **2021**, *22*, 11075. [[CrossRef](#)]
21. Li, W.; Feng, Z.; Sternberg, P.W.; Xu, X.Z. A *C. elegans* stretch receptor Neuron revealed by a mechanosensitive TRP channel homologue. *Nature* **2006**, *440*, 684–687. [[CrossRef](#)]
22. Laing, R.J.; Dhaka, A. ThermoTRPs and Pain. *Neuroscientist* **2016**, *22*, 171–187. [[CrossRef](#)]
23. Almaraz, L.; Manenschijn, J.A.; Peña, E.D.L.; Viana, F. TRPM8. In *Mammalian Transient Receptor Potential (TRP) Cation Channels*; Nilius, B., Flockerzi, V., Eds.; Springer: Berlin/Heidelberg, Germany, 2014; Volume 222, pp. 547–579.
24. Zimmermann, K.; Lennerz, J.K.; Hein, A.; Link, A.S.; Kaczmarek, J.S.; Delling, M.; Uysal, S.; Pfeifer, J.D.; Riccio, A.; Clapham, D.E. Transient receptor potential cation channel, subfamily C, member 5 (TRPC5) is a cold-transducer in the peripheral nervous system. *Proc. Natl. Acad. Sci. USA* **2011**, *108*, 18114–18119. [[CrossRef](#)] [[PubMed](#)]
25. Zygmunt, P.M.; Högestätt, E.D. TRPA1. *Handb. Exp. Pharmacol.* **2014**, *222*, 583–630. [[PubMed](#)]
26. Caterina, M.J.; Schumacher, M.A. The capsaicin receptor: A heat-activated ion channel in the pain pathway. *Nature* **1997**, *389*, 816–824. [[CrossRef](#)] [[PubMed](#)]
27. Hoffstaetter, L.J.; Bagriantsev, S.N.; Gracheva, E.O. TRPs et al.: A molecular toolkit for thermosensory adaptations. *Pflugers Arch.-Eur. J. Physiol.* **2018**, *470*, 745–759. [[CrossRef](#)] [[PubMed](#)]

28. Samanta, A.; Hughes, T.E.T.; Moiseenkova-Bell, V.Y. Transient receptor potential (TRP) channels. In *Membrane Protein Complexes: Structure and Function*; Subcellular Biochemistry; Harris, J., Boekema, E., Eds.; Springer: Singapore, 2018; Volume 87, pp. 141–165.
29. Nagai, K.; Saitoh, Y.; Saito, S.; Tsutsumi, K. Structure and hibernation-associated expression of the transient receptor potential vanilloid 4 channel (TRPV4) mRNA in the Japanese grass lizard (*Takydromus tachydromoides*). *Zool. Sci.* **2012**, *29*, 185–190. [[CrossRef](#)]
30. Ye, Y.; Zhang, H.; Li, J.; Lai, R.; Yang, S.; Du, W.-G. Molecular sensors for temperature detection during behavioral thermoregulation in turtle embryos. *Curr. Biol.* **2021**, *31*, 2995–3003. [[CrossRef](#)]
31. Yan, C.; Wu, W.; Dong, W.; Zhu, B.; Chang, J.; Lv, Y.; Yang, S.; Li, J.-T. Temperature acclimation in hot-spring snakes and the convergence of cold response. *Innovation* **2022**, *3*, 100295. [[CrossRef](#)]
32. Chen, C.; Chen, H.; Zhang, Y.; Thomas, H.R.; Frank, M.H.; He, Y.; Xia, R. TBtools: An integrative toolkit developed for interactive analyses of big biological data. *Mol. Plant* **2020**, *13*, 1194–1202. [[CrossRef](#)]
33. Mistry, J.; Finn, R.D.; Eddy, S.R.; Bateman, A.; Punta, M. Challenges in homology search: HMMER3 and convergent evolution of coiled-coil regions. *Nucleic Acids Res.* **2013**, *41*, e121. [[CrossRef](#)]
34. Cao, Y.; Li, Y.; Wang, L.; Zhang, L.; Jiang, L. Evolution and function of ubiquitin-specific proteases (UBPs): Insight into seed development roles in plants. *Int. J. Biol. Macromol.* **2022**, *221*, 796–805. [[CrossRef](#)]
35. Lu, S.; Wang, J.; Chitsaz, F.; Derbyshire, M.K.; Geer, R.C.; Gonzales, N.R.; Gwadz, M.; Hurwitz, D.I.; Marchler, G.H.; Song, J.S.; et al. CDD/SPARCLE: The conserved domain database in 2020. *Nucleic Acids Res.* **2020**, *48*, D265–D268. [[CrossRef](#)] [[PubMed](#)]
36. Lin, Y.; Xiao, Q.; Hao, Q.; Qian, Z.; Li, X.; Li, P.; Li, H.; Chen, L. Genome-wide identification and functional analysis of the glutathione S-transferase (GST) family in *Pomacea canaliculate*. *Int. J. Biol. Macromol.* **2021**, *193*, 2062–2069. [[CrossRef](#)] [[PubMed](#)]
37. Bailey, T.L.; Johnson, J.; Grant, C.E.; Noble, W.S. The MEME Suite. *Nucleic Acids Res.* **2015**, *43*, W39–W49. [[CrossRef](#)]
38. Bailey, T.L.; Boden, M.; Buske, F.A.; Frith, M.; Grant, C.E.; Clementi, L.; Ren, J.; Li, W.W.; Noble, W.S. MEME Suite: Tools for motif discovery and searching. *Nucleic Acids Res.* **2009**, *37*, W202–W208. [[CrossRef](#)] [[PubMed](#)]
39. Venkatachalam, K.; Montell, C. TRP channels. *Annu. Rev. Biochem.* **2007**, *76*, 387–417. [[CrossRef](#)]
40. Katoh, K.; Kuma, K.; Toh, H.; Miyata, T. MAFFT version 5: Improvement in accuracy of multiple sequence alignment. *Nucleic Acids Res.* **2005**, *33*, 511–518. [[CrossRef](#)] [[PubMed](#)]
41. Zhang, D.; Gao, F.; Jakovlić, I.; Zou, H.; Zhang, J.; Li, W.X.; Wang, G.T. PhyloSuite: An integrated and scalable desktop platform for streamlined molecular sequence data management and evolutionary phylogenetics studies. *Mol. Ecol. Res.* **2020**, *20*, 348–355. [[CrossRef](#)]
42. Minh, B.Q.; Schmidt, H.A.; Chernomor, O.; Schrempf, D.; Woodhams, M.D.; von Haeseler, A.; Lanfear, R. IQ-TREE 2: New models and efficient methods for phylogenetic inference in the genomic era. *Mol. Biol. Evol.* **2020**, *37*, 1530–1534. [[CrossRef](#)]
43. Letunic, I.; Bork, P. Interactive Tree of Life (iTOL) v5: An online tool for phylogenetic tree display and annotation. *Nucleic Acids Res.* **2021**, *49*, W293–W296. [[CrossRef](#)]
44. Emms, D.M.; Kelly, S. OrthoFinder: Phylogenetic orthology inference for comparative genomics. *Genome Biol.* **2019**, *20*, 238. [[CrossRef](#)]
45. Wang, Y.; Tang, H.; Debarry, J.D.; Tan, X.; Li, J.; Wang, X.; Lee, T.H.; Jin, H.; Marler, B.; Guo, H.; et al. MCScanX: A toolkit for detection and evolutionary analysis of gene synteny and collinearity. *Nucleic Acids Res.* **2012**, *40*, e49. [[CrossRef](#)]
46. Chen, C.; Wu, Y.; Xia, R. A painless way to customize circos plot: From data preparation to visualization using TBtools. *iMeta* **2022**, *1*, e35. [[CrossRef](#)]
47. Lezama-García, K.; Mota-Rojas, D.; Pereira, A.M.F.; Martínez-Burnes, J.; Ghezzi, M.; Domínguez, A.; Gómez, J.; de Mira Geraldo, A.; Lendez, P.; Hernández-Ávalos, I.; et al. Transient receptor potential (TRP) and thermoregulation in animals: Structural biology and neurophysiological aspects. *Animals* **2022**, *12*, 106. [[CrossRef](#)] [[PubMed](#)]
48. Gao, F.; Chen, C.; Arab, D.A.; Du, Z.; He, Y.; Ho, S.Y.W. EasyCodeML: A visual tool for analysis of selection using CodeML. *Ecol. Evol.* **2019**, *9*, 3891–3898. [[CrossRef](#)] [[PubMed](#)]
49. Zhang, L.; Liu, G.; Xia, T.; Yang, X.; Sun, G.; Zhao, C.; Xu, C.; Zhang, H. Evolution of toll-like receptor gene family in amphibians. *Int. J. Biol. Macromol.* **2022**, *208*, 463–474. [[CrossRef](#)]
50. Pond, S.L.K.; Frost, S.D.W. Datamonkey: Rapid detection of selective pressure on individual sites of codon alignments. *Bioinformatics* **2005**, *21*, 2531–2533. [[CrossRef](#)]
51. Swanson, W.J.; Nielsen, R.; Yang, Q. Pervasive adaptive evolution in mammalian fertilization proteins. *Mol. Biol. Evol.* **2003**, *20*, 18–20. [[CrossRef](#)]
52. Yang, Z.; Wong, W.S.; Nielsen, R. Bayes empirical Bayes inference of amino acid sites under positive selection. *Mol. Biol. Evol.* **2005**, *22*, 1107–1118. [[CrossRef](#)]
53. Deakin, J.E.; Ezaz, T. Understanding the evolution of reptile chromosomes through applications of combined cytogenetics and genomics approaches. *Cytogenet. Genome Res.* **2019**, *157*, 7–20. [[CrossRef](#)]
54. Himmel, N.J.; Cox, D.N. Transient receptor potential channels: Current perspectives on evolution, structure, function and nomenclature. *Proc. R. Soc. B.* **2020**, *287*, 20201309. [[CrossRef](#)]
55. Wang, H.; Siemens, J. TRP ion channels in thermosensation, thermoregulation and metabolism. *Temperature* **2015**, *2*, 178–187. [[CrossRef](#)] [[PubMed](#)]
56. England, S.J.; Campbell, P.C.; Banerjee, S.; Swanson, A.J.; Lewis, K.E. Identification and expression analysis of the complete family of zebrafish pkd genes. *Front. Cell Dev. Biol.* **2017**, *5*, 5. [[CrossRef](#)] [[PubMed](#)]

57. Maher, C.; Stein, L.; Ware, D. Evolution of Arabidopsis microRNA families through duplication events. *Genome Res.* **2006**, *16*, 510–519. [[CrossRef](#)] [[PubMed](#)]
58. Buckley, L.B.; Schoville, S.D.; Williams, C.M. Shifts in the relative fitness contributions of fecundity and survival in variable and changing environments. *J. Exp. Biol.* **2021**, *224*, jeb228031. [[CrossRef](#)]
59. Vazquez, C.; Rowcliffe, J.M.; Spoelstra, K.; Jansen, P.A. Comparing diel activity patterns of wildlife across latitudes and seasons: Time transformations using day length. *Methods Ecol. Evol.* **2019**, *10*, 2057–2066. [[CrossRef](#)]
60. Gamble, T.; Greenbaum, E.; Jackman, T.R.; Bauer, A.M. Into the light: Diurnality has evolved multiple times in geckos. *Biol. J. Linn. Soc.* **2015**, *115*, 896–910. [[CrossRef](#)]
61. Meiri, S.; Bauer, A.M.; Chirio, L.; Colli, G.R.; Das, I.; Doan, T.M.; Feldman, A.; Herrera, F.-C.; Novosolov, M.; Pafilis, P.; et al. Are lizards feeling the heat? A tale of ecology and evolution under two temperatures. *Glob. Ecol. Biogeogr.* **2013**, *22*, 834–845. [[CrossRef](#)]
62. Moreira, M.O.; Qu, Y.-F.; Wiens, J.J. Large-scale evolution of body temperatures in land vertebrates. *Evol. Lett.* **2021**, *5*, 484–494. [[CrossRef](#)]
63. Redman, L.M.; Smith, S.R.; Burton, J.H.; Martin, C.K.; Il'yasova, D.; Ravussin, E. Metabolic slowing and reduced oxidative damage with sustained caloric restriction support the rate of living and oxidative damage theories of aging. *Cell Metab.* **2018**, *27*, 805–815.e4. [[CrossRef](#)]
64. Brauchi, S.; Orio, P.; Latorre, R. Clues to understanding cold sensation: Thermodynamics and electrophysiological analysis of the cold receptor TRPM8. *Proc. Natl. Acad. Sci. USA* **2004**, *101*, 15494–15499. [[CrossRef](#)]